

## Efficient Analysis of Nonviable Poliovirus Capsid Mutants

JOHN SIMONS,<sup>1</sup> ANDREW ROGOVE,<sup>2†</sup> NICOLA MOSCUFO,<sup>2‡</sup>  
CAROL REYNOLDS,<sup>1§</sup> AND MARIE CHOW<sup>2\*</sup>

*Departments of Applied Biological Sciences<sup>1</sup> and Biology,<sup>2</sup> Massachusetts  
Institute of Technology, Cambridge, Massachusetts 02139*

Received 28 September 1992/Accepted 10 December 1992

**Nonviable poliovirus capsid mutants were studied by an efficient infection-transfection system. Phenotypically, nonviable poliovirus capsid mutants appear to segregate into three classes: those that form only protomers, those that can form pentamers, and one that can form completed virions.**

The ability to construct site-specific mutations within genomic cDNA clones of RNA viruses has yielded a wealth of information on viral gene function. Through the use of standard recombinant techniques, construction of viable and conditional lethal poliovirus mutants has enabled the effects on viral infection, genome replication, immune avoidance, and host pathology of specific amino acid or nucleotide substitutions to be examined. However, site-specific mutagenesis studies have generated additional nonviable poliovirus clones (7, 8, 12, 16, 18, 19). Although the mutations leading to these nonviable viruses demonstrate the importance of specific protein and/or nucleic acid residues, it has been difficult to identify the replication stages affected in these mutants. These difficulties are in part technical, stemming from the low efficiencies typically observed upon transfection of plasmids containing the mutant cDNAs or RNA transcripts and/or the asynchrony of viral gene expression observed after transfection. Here we describe an efficient transient transfection system that allows the study of nonviable poliovirus capsid mutants.

**Transfection of poliovirus cDNAs.** Transfection of poliovirus cDNAs utilized the high transfection efficiency afforded by electroporation (4); the plasmid pPVM-1, which contained an infectious cDNA copy of the poliovirus genome (serotype 1, Mahoney strain) downstream of a bacteriophage T7 RNA promoter (17, 20); and the expression of T7 RNA polymerase from a recombinant vaccinia virus, vTF7-3 (5). HeLa cells, maintained in suspension, were pelleted and resuspended at a concentration of  $5 \times 10^6$  cells per ml in Joklik-minimum essential medium (GIBCO)-20 mM HEPES (*N*-2-hydroxyethylpiperazine-*N'*-2-ethanesulfonic acid) (pH 7.2)-0.1% bovine serum albumin. Cells were infected with sucrose-purified vTF7-3 at a multiplicity of infection of 20. Virus was allowed to adsorb for 60 min at 37°C with gentle shaking every 10 to 15 min. Plasmid pPVM-1 (20 µg/ml with 60 µg of salmon sperm DNA per ml as a carrier) was transfected into vTF7-3-infected HeLa cells ( $2 \times 10^6$  cells per 0.4 ml) with an electroporation device (BTX Electro Cell Manipulator 600) set at 170 to 175 V (delivering a field strength of 0.68 to 0.7 kV/cm), 13 Ω, and 1,650 µF, using 2-mm-gap electroporation cuvettes (Bio-Rad). (The electro-

poration conditions were determined to be yielding optimal transfection efficiencies with approximately 30% cell viability [4]. For unknown reasons, if poliovirus infection is initiated after 4 h post-vaccinia virus infection, poliovirus replication is inhibited [as detected by plaque production]. If poliovirus infection is initiated within 2 h post-vaccinia virus infection, no inhibition of poliovirus replication is observed; rather, vaccinia virus replication is inhibited [15a]. Thus, the timing of the transfection is likely to be important for the overall efficiency of poliovirus expression.) The transfected cells were incubated at room temperature for 10 min, subsequently plated into tissue culture dishes in Dulbecco's modified Eagle's medium (GIBCO) without methionine supplemented with 5% fetal bovine serum, and incubated at 37°C, 5% CO<sub>2</sub>. At 4 h posttransfection, medium and nonadherent cells were aspirated from the plates and fresh medium containing [<sup>35</sup>S]methionine (50 µCi/ml; specific activity, 1,170 Ci/mmol; NEN) was added. Cells were harvested at 7 h posttransfection and lysed in RIPA buffer (10 mM Tris [pH 7.5], 150 mM NaCl, 1% deoxycholate, 1% Triton X-100, 0.1% sodium dodecyl sulfate [SDS]), and total cellular protein was measured (Pierce protein assay). Cell lysates (10 µg each) were subjected to electrophoresis through an SDS-10% polyacrylamide gel and transferred onto nitrocellulose filters. These were analyzed by autoradiography (Fig. 1).

Cells infected with vaccinia virus vTF7-3 and transfected with plasmid pPVM-1 (vTF7-3-infected/pPVM-1-transfected cells) produce the same protein profile as that observed for wild-type poliovirus-infected cells, with a few additional vaccinia virus-specific proteins (Fig. 1, lanes 2 and 4). The identities of poliovirus-specific bands seen in the autoradiograph were confirmed by Western blot (immunoblot) analysis (data not shown). The inclusion of dactinomycin (5 µg/ml) at 2 h posttransfection strongly reduced both poliovirus protein and background protein bands. Consistent with poliovirus transcription being driven initially from the T7 promoter and with the kinetics of T7 RNA polymerase expression from the vaccinia virus vTF7-3 vector (5), DNA-dependent RNA synthesis is necessary for more than 2 h posttransfection to provide sufficient templates for poliovirus RNA and protein synthesis. The relatively low amount of background cellular protein synthesis observed most likely results from the shutoff of host protein synthesis that occurs in both vaccinia virus- and poliovirus-infected cells. The low background of cellular protein synthesis allowed the production of poliovirus-specific proteins to be directly assessed in labeled cell lysates without additional analyses by immunoprecipitations or Western blots. The efficiency of the cou-

\* Corresponding author.

† Present address: School of Medicine, State University of New York at Stony Brook, Stony Brook, NY 11794.

‡ Present address: Department of Dermatology, Tufts University Medical School, Boston, MA 02111.

§ Present address: Department of Pathology, Brigham and Women's Hospital, Boston, MA 02115.

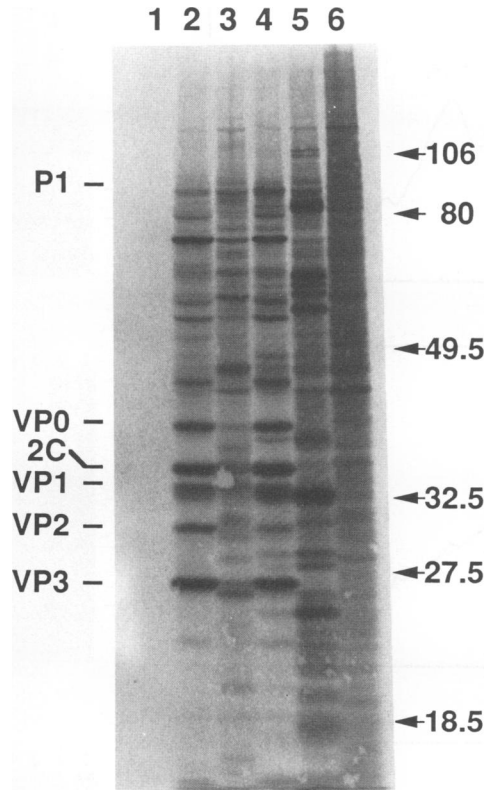


FIG. 1. HeLa cells infected with vTF7-3 and transfected with pPVM-1 express poliovirus proteins. Lysates from infected-transfected cells (10  $\mu$ g of protein per well) were separated on a 10% polyacrylamide gel and electroblotted onto a nitrocellulose membrane. The membrane was then subjected to autoradiography (2 days at  $-70^{\circ}\text{C}$ ). Lanes: 1, prestained standards; 2, poliovirus-infected HeLa cell lysates (labeled from 3 to 5 h postinfection); 3, vTF7-3-infected/pPVM-1-transfected cells treated with dactinomycin at 2 h posttransfection; 4, vTF7-3-infected/pPVM-1-transfected cells; 5, cells infected only with vTF7-3; 6, cells that were mock infected and transfected with pPVM-1. The positions of the capsid protein precursor, P1; capsid proteins; and prestained molecular mass markers (in kilodaltons) are indicated.

pled vaccinia virus infection-cDNA transfection system is also reflected by the high percentage of cells producing virus upon transfection of the infectious wild-type pPVM-1 plasmid; approximately 30 to 35% of the viable cells (i.e., 10% of the electroporated cells) release infectious virus as measured by infectious center assays (data not shown).

The low background of labeled host and vaccinia virus proteins allowed the poliovirus capsid assembly intermediates formed in transfected cells to be examined directly on sucrose gradients (15). The major assembly products (5S protomers, 14S pentamers, 73S empty capsids, and 150S mature virions) are present in labeled lysates from vTF7-3-infected/pPVM-1-transfected cells (Fig. 2A). SDS-polyacrylamide gel analysis of the peak fractions from the gradients displays the expected VP0-VP1-VP3 protein composition for the various assembly intermediates. In addition, the 150S particles are infectious and are indistinguishable from sucrose-purified, mature virions obtained from wild-type-infected HeLa cells. Thus, the poliovirus assembly pathway observed in the coupled poliovirus plasmid transfection-vTF7-3 infection system recapitulates that which is observed

during poliovirus infection and enables the assembly of nonviable poliovirus capsid mutants to be analyzed with an ease comparable to that for viable viral mutants.

**Analyses of nonviable poliovirus capsid mutants.** Analyses of nonviable poliovirus capsid mutants using the described infection-transfection technique were undertaken to determine at which stage in the assembly pathway nonviable mutants were blocked. Previous site-specific substitutions in residues that form the myristoylation signal sequence (18), form neutralization site 3B (16), or interact with the myristate moiety (12) have produced poliovirus mutants which upon transfection of the mutant cDNA plasmids themselves or genomic RNA transcripts of the cDNA plasmids produced no plaques. Characterization of these nonviable mutants has not been achievable by previously published methods (6, 10). Study of viable mutants obtained from these mutagenesis studies suggested that critical points in the poliovirus replicative cycle were affected. Mutations in the myristate signal sequence reduced the levels of myristate modification on capsid protein VP4 precursors. This, in turn, affected proper assembly of pentamers and empty capsids (14). Mutations of highly conserved, solvent-exposed surface residues in antigenic site 3B (which spans a pentamer-pentamer boundary) disturbed P1 (uncleaved protomer) folding (15). Finally, mutations which affect interprotomer myristate-protein interactions, in comparison to wild-type virus, resulted in an accumulation of 14S pentamers in infected cells and reduced levels of infectivity and thermostability (12). But because these "viable" substitutions do not inhibit completely the formation of infectious virus, it has been difficult to identify the site(s) at which the mutation affects the viral replicative cycle. In contrast, characterization of nonviable mutants allows the rapid identification of any severe blocks present in the assembly pathway of these viruses.

Wild-type and mutant pPVM-1 plasmids were transfected into vaccinia virus vTF7-3-infected HeLa cells ( $1 \times 10^7$  to  $2 \times 10^7$  cells). Lysates from [ $^{35}\text{S}$ ]methionine-labeled cells were prepared (14) and analyzed by SDS-polyacrylamide gel electrophoresis. Lysates from cells transfected with nonviable mutants containing substitutions that alter the myristoylation signal sequence, neutralization site 3B, or myristate-protein interactions showed protein profiles comparable to that from the wild-type-transfected cells, indicating that capsid protein processing in these mutants was not significantly affected (Fig. 2B, C, and D and data not shown). Thus, the lethal defect for each of these groups of nonviable capsid mutants does not appear to be due to defects in protein synthesis and/or processing.

Sucrose gradient analysis of assembly intermediates found in the transfected cells demonstrates the existence of three different classes of nonviable mutants (Table 1): those that can form only 5S protomers (e.g., 4002G.A [Fig. 2B]), those that form only 5S protomers and 14S pentamers (e.g., 2246E.R [Fig. 2C]), and one that forms fully assembled virions (4028T.G [Fig. 2D]). With the exception of mutants with substitutions at Thr-28 of VP4 (4028T), the phenotypes of the nonviable mutants are generally consistent with predictions based on analysis of the assembled virion structure. The myristate moiety is located at the fivefold axis. Elimination of this modification by destroying the myristoylation signal sequence prevents the assembly of 14S pentamers. These results agree with studies by Ansardi et al. (2) using recombinant vaccinia virus-poliovirus expression vectors. Because unmodified protomers can be incorporated into pentamer and empty-capsid intermediates in the presence of

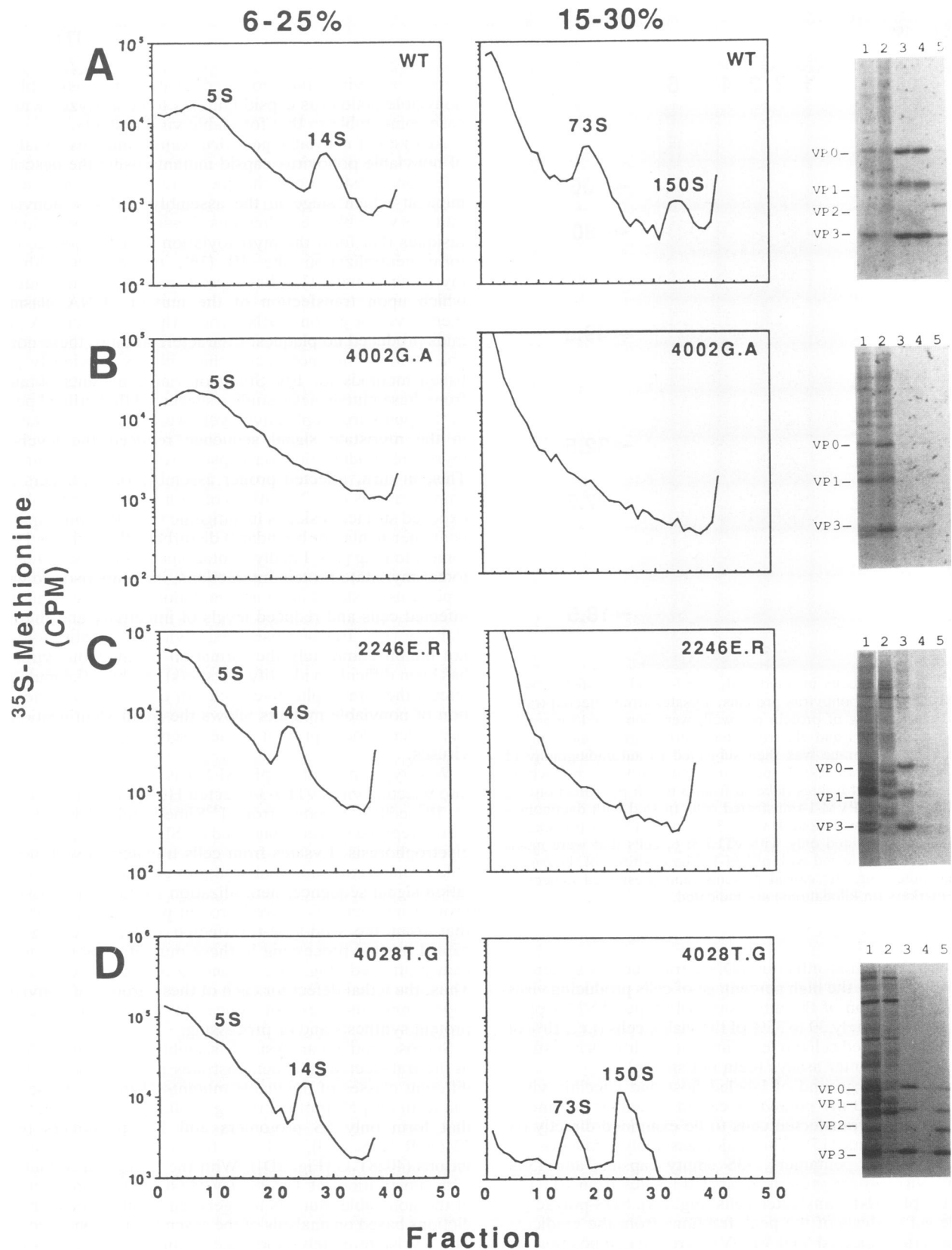


FIG. 2. Analysis of assembly intermediates present in wild-type- and nonviable poliovirus mutant-transfected cells. Lysates from wild-type- (A) and from 4002G.A (B), 2246E.R (C), and 4028T.G (D) poliovirus-transfected cells were analyzed by standard sucrose gradient techniques (15). The positions of the 5S protomers, 14S pentamers, 73S empty capsids, and 150S mature virions were identified in a gradient containing the wild-type-transfected lysates which was run in parallel with the gradients containing the mutant lysate during each centrifugation. Autoradiographs of an unenhanced gel of the peak fractions are displayed on the right of the figure. Lanes 1, unfractionated lysate; lanes 2, 5S region; lanes 3, 14S region; lanes 4, 73S region; lanes 5, 150S region. The 4028T.G profile was generated by fractionating the entire lysate on a 6 to 25% sucrose gradient, after which the pellet from this gradient was resuspended and separated on a 15 to 30% sucrose gradient.

TABLE 1. Analysis of nonviable poliovirus capsid mutants

Mutant <sup>a</sup>	Largest intermediate <sup>b</sup>	Site of mutation <sup>c</sup>
4002G.A (GCG)	5S	Myristoyl signal sequence
4002G.V (GTG)	5S	Myristoyl signal sequence
4002G.M (ATG)	5S	Myristoyl signal sequence
4002G.Y (TAC)	5S	Myristoyl signal sequence
4002G.E (GAG)	5S	Myristoyl signal sequence
4002G.R (CGG)	5S	Myristoyl signal sequence
2074E.K (AAA)	14S	Neutralization site 3B
2243S.P (CCG)	14S	Neutralization site 3B
2246E.R (CGC)	14S	Neutralization site 3B
4028T.K (CGG)	14S	Myristate-protein interactions
4028T.G (GGG)	150S	Myristate-protein interactions

<sup>a</sup> Mutant nomenclature: the number and letters identify the location and amino acid substitution within the poliovirus genome. The first number refers to the capsid protein in which the mutation is located; the following three numbers refer to the amino acid residue position; the final two letters refer to the wild-type and mutant residues, respectively. In addition, the mutated codon is reported in parentheses. Therefore, 4002G.A, for example, is a substitution of an alanine for the wild-type glycine at the second residue (counting from the N-terminal methionine) of VP4. Wild-type codons are 4002 (GGT), 2074 (GAG), 2243 (TCG), 2246 (GAG), and 4028 (ACC).

<sup>b</sup> Fastest-sedimenting (i.e., most complete) assembly intermediate found by sucrose gradient analysis of infected-transfected cell lysates.

<sup>c</sup> Proposed disturbance caused by the mutation.

myristoyl-modified protomers (14), the myristoyl moiety may catalyze the nucleation of pentamers and stabilize this structure. Thus, the small amount of 14S and 73S assembly intermediates previously observed for these nonviable mutants (9, 10) may have resulted from the presence of a low level of myristoyl-modified revertants, as a single base transversion restores the wild-type codon. Neutralization site 3B is formed from residues that span pentamer-pentamer boundaries. The nonviable mutants containing substitutions at these residues appear to assemble pentamer structures but fail to assemble pentamers into empty capsids. Thus, mutations near the pentamer-pentamer boundary prevent the assembly of 14S pentamers into larger structures. The phenotypes of the nonviable 4028T mutants were unexpected. The threonine 28 residue of VP4 forms an interprotomer hydrogen bond between its hydroxyl moiety and the carbonyl oxygen of a neighboring myristate (3). This hydrogen bond has been hypothesized to stabilize the pentamer subunit structure. Surprisingly, 4028T.K can form 5S protomers and 14S pentamers even though the mutation drastically changes the chemical properties at this residue position. Even more unexpected was the phenotype of the 4028T.G mutant. 4028T.G forms complete virions that are similar to wild-type virions by several biochemical criteria (13). The exact nature of the lethal defect remains to be identified. However, the presence of a 150S particle containing VP2 indicates that these particles package RNA.

The ability to study nonviable virus mutants allows one to examine how essential genes function in a virus's replicative cycle. Three methods for examining nonviable poliovirus clones have been published previously. One utilizes *in vitro* translation systems programmed with mutant poliovirus RNA (6, 8, 11). Another method relies on the DEAE-dextran-mediated transfection of *in vitro*-transcribed viral RNA into susceptible cells in an effort to force one cycle of replication (9, 10). A third method allows characterization of the processing and assembly of nonviable capsid mutants by

coinfection of recombinant vaccinia virus vectors expressing poliovirus capsid proteins and 3CD protease (1, 2). The infection-transfection system described here has several advantages over its predecessors: it is very efficient (wild-type cDNA produces approximately  $10^8$  PFU/ $10^7$  HeLa cells originally electroporated), the low level of background cellular protein synthesis allows the direct analysis of labeled viral proteins without additional immunoprecipitations or Western analyses, and nonviable clones can be analyzed directly without having to construct a comparable mutation in a vaccinia virus vector.

By using this method to study nonviable capsid mutants, three classes of mutants have been identified: those that cannot assemble 14S and larger structures, those that cannot assemble 73S and larger structures, and one that assembles completed virions that are not infectious. Although only a small number of mutants have been examined to date, it is likely that further studies will identify RNA packaging mutants which assemble 5S, 14S, and 73S structures but do not form 150S virions. In addition, this general methodology may be applicable to the characterization of nonviable virus arising from mutations in other regions of the poliovirus genome.

We thank Rich Condit for initial help with the vaccinia virus technology, Dan Treiber and Jill Mello for assistance with the electroporations, and Ed Niles for supplying vTF7-3.

This work was supported by Public Health Service grant AI122627 from NIH and by research grant MV-466 from the American Cancer Society.

#### REFERENCES

1. Ansardi, D. C., D. C. Porter, and C. D. Morrow. 1991. Coinfection with recombinant vaccinia viruses expressing poliovirus P1 and P3 proteins results in polyprotein processing and formation of empty capsid structures. *J. Virol.* **65**:2088-2092.
2. Ansardi, D. C., D. C. Porter, and C. D. Morrow. 1992. Myristylation of poliovirus capsid precursor P1 is required for assembly of subviral particles. *J. Virol.* **66**:4556-4563.
3. Chow, M., J. F. E. Newman, D. Filman, J. M. Hogle, D. J. Rowlands, and F. Brown. 1987. Myristylation of picornavirus capsid protein VP4 and its structural significance. *Nature (London)* **327**:482-486.
4. Chu, G., H. Hayakawa, and P. Berg. 1987. Electroporation for the efficient transfection of mammalian cells with DNA. *Nucleic Acids Res.* **15**:1311-1325.
5. Fuerst, T. R., E. G. Niles, F. W. Studier, and B. Moss. 1986. Eukaryotic transient-expression system based on recombinant vaccinia virus that synthesizes bacteriophage T7 RNA polymerase. *Proc. Natl. Acad. Sci. USA* **83**:8122-8126.
6. Kräusslich, H.-G., C. Hölscher, Q. Reuer, J. Harber, and E. Wimmer. 1990. Myristoylation of the poliovirus polyprotein is required for proteolytic processing of the capsid and for viral infectivity. *J. Virol.* **64**:2433-2436.
7. Kuhn, R. J., H. Tada, M. F. Ypma-Wong, J. J. Dunn, B. L. Semler, and E. Wimmer. 1988. Construction of a "mutagenesis cartridge" for poliovirus genome-linked protein: isolation and characterization of viable and nonviable mutants. *Proc. Natl. Acad. Sci. USA* **85**:519-523.
8. Marc, D., G. Dugeon, A. Haenni, M. Girard, and S. van der Werf. 1989. Role of myristoylation of poliovirus capsid protein VP4 as determined by site-directed mutagenesis of its N-terminal sequence. *EMBO J.* **8**:2661-2668.
9. Marc, D., M. Girard, and S. van der Werf. 1991. A glycine to ALA substitution in poliovirus capsid protein VP0 blocks its myristoylation and prevents viral assembly. *J. Gen. Virol.* **72**:1151-1157.
10. Marc, D., G. Masson, M. Girard, and S. van der Werf. 1990. Lack of myristoylation of poliovirus capsid polypeptide VP0 prevents the formation of virions or results in the assembly of

- noninfectious virus particles. *J. Virol.* **64**:4099–4107.
11. **Molla, A., A. V. Paul, and E. Wimmer.** 1991. Cell-free de novo synthesis of poliovirus. *Science* **254**:1647–1651.
  12. **Moscufo, N., and M. Chow.** 1992. Myristate-protein interactions in poliovirus: interactions of VP4 threonine 28 contribute to the structural conformation of assembly intermediates and the stability of assembled virions. *J. Virol.* **66**:6849–6857.
  13. **Moscufo, N., and M. Chow.** Unpublished observations.
  14. **Moscufo, N., J. Simons, and M. Chow.** 1991. Myristoylation is important at multiple stages in poliovirus assembly. *J. Virol.* **65**:2372–2380.
  15. **Reynolds, C., D. Birnby, and M. Chow.** 1992. Folding and processing of the capsid protein precursor P1 is kinetically retarded in neutralization site 3B mutants of poliovirus. *J. Virol.* **66**:1641–1648.
  - 15a. **Reynolds, C., and M. Chow.** Unpublished observations.
  16. **Reynolds, C., G. Page, H. Zhou, and M. Chow.** 1991. Identification of residues in VP2 that contribute to poliovirus neutralization antigenic site 3B. *Virology* **184**:391–396.
  17. **Sarnow, P.** 1989. Role of 3'-end sequences in infectivity of poliovirus transcripts made in vitro. *J. Virol.* **63**:467–470.
  18. **Simons, J., C. Reynolds, N. Moscufo, L. Curry, and M. Chow.** 1990. Myristylation of poliovirus VP4 capsid proteins, p. 158–165. *In* M. A. Brinton and F. X. Heinz (ed.), *New aspects of positive-strand RNA viruses*. American Society for Microbiology, Washington, D.C.
  19. **Trono, D., R. Andino, and D. Baltimore.** 1988. An RNA sequence of hundreds of nucleotides at the 5' end of poliovirus RNA is involved in allowing viral protein synthesis. *J. Virol.* **62**:2291–2299.
  20. **van der Werf, S., J. Bradley, E. Wimmer, F. W. Studier, and J. J. Dunn.** 1986. Synthesis of infectious poliovirus RNA by purified T7 RNA polymerase. *Proc. Natl. Acad. Sci. USA* **83**:2330–2334.